

# Electric-field control of local ferromagnetism using a magnetoelectric multiferroic

YING-HAO CHU<sup>1,2,3\*</sup>, LANE W. MARTIN<sup>1,3\*†</sup>, MIKEL B. HOLCOMB<sup>2,3</sup>, MARTIN GAJEK<sup>2</sup>, SHU-JEN HAN<sup>4</sup>, QING HE<sup>2</sup>, NINA BALKE<sup>2</sup>, CHAN-HO YANG<sup>2</sup>, DONKOUN LEE<sup>4</sup>, WEI HU<sup>4</sup>, QIAN ZHAN<sup>1,2</sup>, PEI-LING YANG<sup>1,2</sup>, ARANTXA FRAILE-RODRÍGUEZ<sup>5</sup>, ANDREAS SCHOLL<sup>6</sup>, SHAN X. WANG<sup>4</sup> AND R. RAMESH<sup>1,2,3</sup>

<sup>1</sup>Department of Materials Science and Engineering, University of California, Berkeley, Berkeley, California 94720, USA

<sup>2</sup>Department of Physics, University of California, Berkeley, Berkeley, California 94720, USA

<sup>3</sup>Materials Science Division, Lawrence Berkeley National Laboratory, Berkeley, California 94720, USA

<sup>4</sup>Department of Materials Science and Engineering, Stanford University, Palo Alto, California 94305, USA

<sup>5</sup>Swiss Light Source, Paul Scherrer Institut, Villigen PSI, CH-5232, Switzerland

<sup>6</sup>Advanced Light Source, Lawrence Berkeley National Laboratory, Berkeley, California 94720, USA

\*These authors contributed equally to this work

†e-mail: lwmartin@berkeley.edu

Published online: 27 April 2008; doi:10.1038/nmat2184

Multiferroics are of interest for memory and logic device applications, as the coupling between ferroelectric and magnetic properties enables the dynamic interaction between these order parameters. Here, we report an approach to control and switch local ferromagnetism with an electric field using multiferroics. We use two types of electromagnetic coupling phenomenon that are manifested in heterostructures consisting of a ferromagnet in intimate contact with the multiferroic BiFeO<sub>3</sub>. The first is an internal, magnetoelectric coupling between antiferromagnetism and ferroelectricity in the BiFeO<sub>3</sub> film that leads to electric-field control of the antiferromagnetic order. The second is based on exchange interactions at the interface between a ferromagnet (Co<sub>0.9</sub>Fe<sub>0.1</sub>) and the antiferromagnet. We have discovered a one-to-one mapping of the ferroelectric and ferromagnetic domains, mediated by the colinear coupling between the magnetization in the ferromagnet and the projection of the antiferromagnetic order in the multiferroic. Our preliminary experiments reveal the possibility to locally control ferromagnetism with an electric field.

Electric-field control of ferromagnetism is an exciting new area of condensed-matter research with the potential to impact magnetic data storage, spintronics and high-frequency magnetic devices. Magnetoelectric multiferroics, or materials that simultaneously show some form of magnetic and ferroelectric order, such as BiFeO<sub>3</sub> (BFO) (ref. 1), have piqued the interest of researchers worldwide with the promise of coupling between magnetic and electric order parameters<sup>2,3</sup>. BFO is an antiferromagnetic, ferroelectric multiferroic with a Curie temperature of ~820 °C and a Néel temperature of ~370 °C (refs 4,5). It has been the focus of many papers and much has been learned about how to control the ferroelectric domain structure<sup>6</sup>, the domain switching mechanisms<sup>7</sup>, and, in turn, the coupling between ferroelectric and antiferromagnetic order parameters<sup>8,9</sup>. With these findings in hand, we are exploring a particular manifestation of this multiferroic order in enabling electrical control of magnetism through exchange coupling with a ferromagnet.

At the same time, great advances in exchange interactions at interfaces have occurred since the discovery of this phenomenon in 1956 (refs 10,11). There are two general manifestations of exchange interactions that have been observed at the interface between a ferromagnet and an antiferromagnet. The first is an exchange bias of the magnetic hysteresis loop that is a consequence of pinned, uncompensated spins at the interface; the second is an enhancement of the coercive field of the ferromagnet as a

consequence of enhanced spin viscosity or a ‘spin drag’ effect. Conventional antiferromagnets, such as IrMn, NiO and CoO, do not have the ability to be tuned with an electric field; however, multiferroics such as BFO may offer exactly such an opportunity to gain electrical control of exchange interactions. Studies done on multiferroic materials including YMnO<sub>3</sub> (refs 12,13) and BFO (refs 14–16) show that strong exchange interactions can be demonstrated in a static manner. Borisov *et al.* have proposed an alternative approach in which a magnetoelectric substrate can be used under various cooling treatments with combinations of electric and magnetic fields to effect changes on the exchange field in Cr<sub>2</sub>O<sub>3</sub>(111)/(Co/Pt)<sub>3</sub> heterostructures<sup>17</sup>. Dynamic switching of the exchange field with an applied electric field, however, had remained elusive until a recent report by Laukhin *et al.* focusing on YMnO<sub>3</sub> at very low temperatures<sup>18</sup>. Here, we report the observation of such electric-field control of local magnetism at room temperature.

Our approach to control and switch the local magnetism with an electric field is based on the presence of two coupling mechanisms (Fig. 1a) present in a ferromagnet–multiferroic heterostructure. The first is the coupling between antiferromagnetic BFO and ferromagnetic Co<sub>0.9</sub>Fe<sub>0.1</sub> (CoFe) (exchange coupling) (Fig. 1b) that leads to a significant enhancement in the coercive field of the ferromagnet compared with that of the ferromagnet alone (black hysteresis loop). Recent

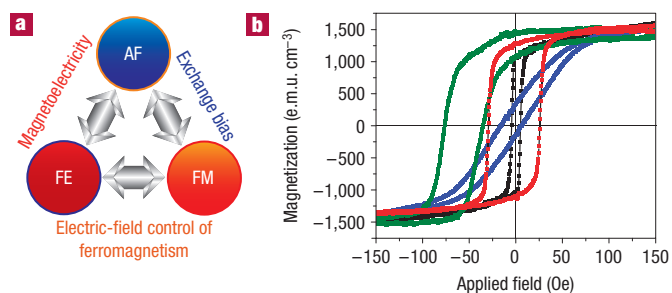


**Figure 1** An approach for electrical control of ferromagnetism. **a**, Schematic diagram showing our method for electrical control of magnetism. The connection between ferroelectricity, antiferromagnetism and ferromagnetism is shown. **b**, Exchange interactions between CoFe and BFO result in either an enhanced coercive field (red and blue data for hysteresis loops measured parallel and perpendicular to growth field, respectively) or an exchange-biased hysteresis loop (green data measured parallel to growth field) for the CoFe layer compared with CoFe grown directly on STO(001) (black data).

findings (L.W.M. *et al.*, manuscript in preparation) reveal the ability to control the nature of such exchange interactions in CoFe/BFO heterostructures, by controlling the relative fractions

of different types of ferroelectric domain wall in the BFO film. Thus, the heterostructure can be controlled to exhibit only an enhancement of the coercive field (red hysteresis loop) or both an enhancement of the coercive field and a shift of the hysteresis loop of the ferromagnet (green hysteresis loop) (Fig. 1b). The second coupling mechanism of importance is between ferroelectricity and antiferromagnetism in the multiferroic BFO (refs 9,19). Building on this ability to control and create exchange interactions between the antiferromagnetic order in BFO and a traditional ferromagnet and the ability to electrically control the antiferromagnetic order in BFO, we have explored the possibility of controlling ferromagnetism with an electric field.

Heterostructures of Au (2 nm)/CoFe (2.5–20 nm)/BFO (50–200 nm)/SrRuO<sub>3</sub> (SRO) (25–50 nm) were grown on SrTiO<sub>3</sub> (STO) (001)-oriented substrates; growth details are presented in the Methods section. The surface structure and underlying ferroelectric domain structure were determined using a combination of atomic force microscopy and piezoresponse force microscopy (PFM) and structural measurements were carried out using scanning transmission electron microscopy (STEM). Atomic-resolution imaging and electron energy-loss spectroscopy (EELS) attest to the high quality of the BFO/CoFe interface. High-angle annular dark-field transmission electron microscopy imaging shows the uniformly high-quality Ta/CoFe/BFO/SRO/STO(001) heterostructures (Fig. 2a). STEM imaging of the Ta/CoFe/BFO interfaces demonstrates that they are smooth and clean at

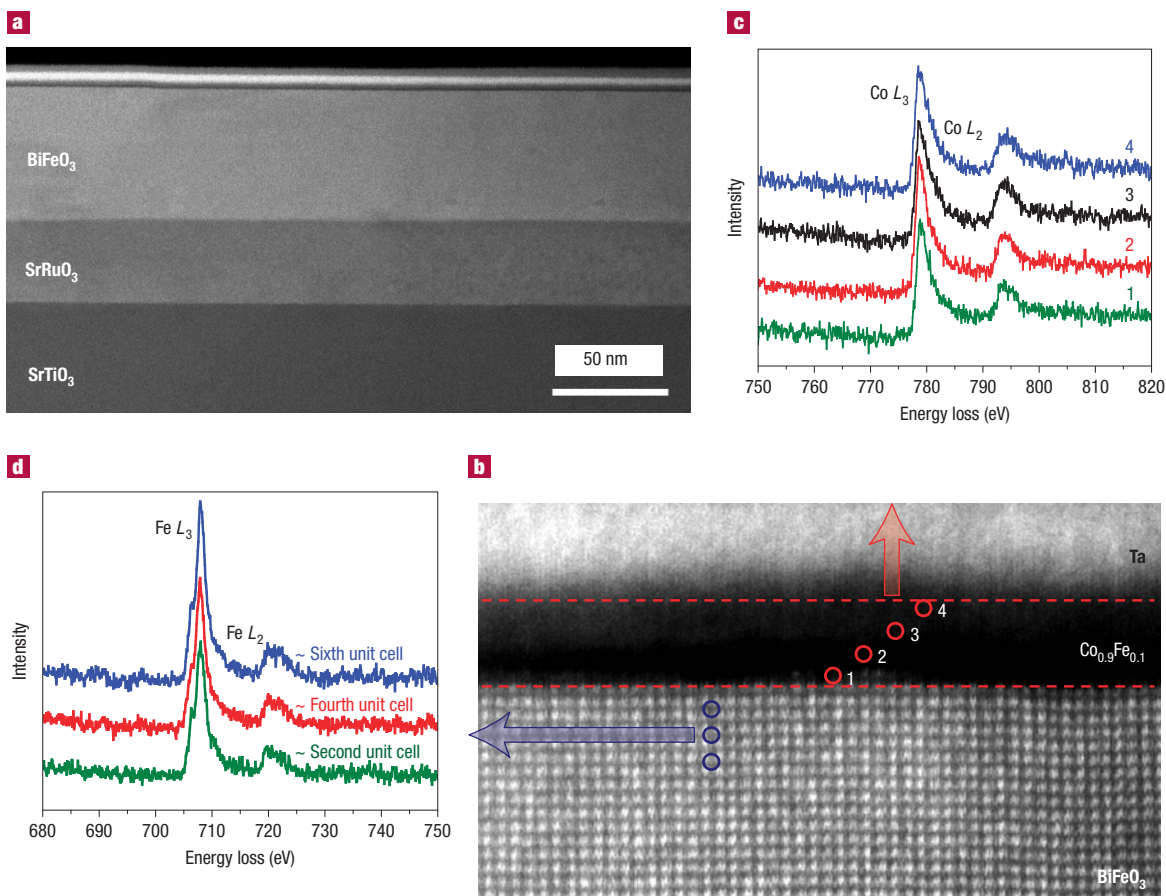


**Figure 2** Structural and chemical characterization of exchange heterostructures. **a**, High-angle annular dark-field image of highly uniform Ta/CoFe/BFO/SRO/STO(001) heterostructure. **b**, STEM image of the interface between CoFe and BFO. Interfaces are smooth and pristine at an atomic level. **c,d**, EELS confirmed that there was neither oxidation of the Co in the CoFe layer (**c**) nor reduction of the Fe in the BFO layer near the interface (**d**).

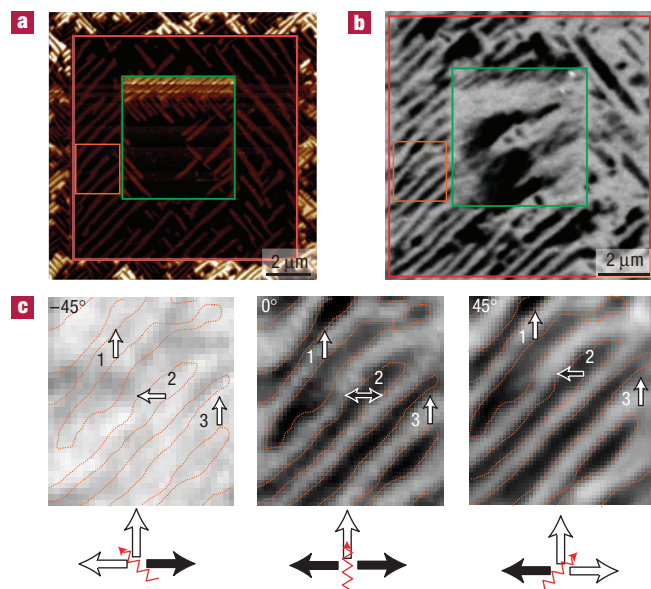


**Figure 3** Microscopic evidence for coupling. **a**, In-plane PFM image showing the ferroelectric domain structure of a BFO film with a large ( $10\ \mu\text{m}$ , red square) and small ( $5\ \mu\text{m}$ , green square) electrically switched region. **b**, Corresponding XMCD-PEEM image taken at the Co  $L$ -edge for a CoFe film grown on the written pattern. Direct matching of domain structures is evident. Black contrast is interpreted as a spin pointing side-to-side in the image and grey as spin pointing up. **c**, Rotation of the sample in reference to the incoming right-circularly polarized light enables full determination of the nature of magnetism in the CoFe layer.

the atomic scale (Fig. 2b). Both STEM and high-resolution transmission electron microscopy analyses suggest that the CoFe and Ta layers are either amorphous or nanocrystalline. Furthermore, the interface between the BFO and CoFe is very smooth and there is no evidence of interdiffusion between the CoFe and BFO and the Ta and CoFe. EELS was completed at various points throughout the CoFe (Fig. 2c) and BFO (Fig. 2d) films and confirms that there has been no oxidation of the CoFe film and no reduction of the Fe in BFO near the interface. Typical BFO/SRO/STO (001) surfaces were found to exhibit an average r.m.s. surface roughness of  $\sim 0.6\ \text{nm}$ .

The promise of this approach to control magnetism with an electric field begins with the use of our ability to selectively control ferroelectric switching events in BFO thin films (Fig. 3a). Using PFM, regions of a BFO film were electrically switched with a set of positive and negative voltages to create a ‘box-in-a-box’ architecture. A  $10\ \mu\text{m}$  region was poled upward with a  $-12\ \text{V}$  applied field (red square), inside of which a smaller  $5\ \mu\text{m}$  region was subsequently poled downward with a  $+12\ \text{V}$  applied field (green square) (Fig. 3a). A  $2.5\text{-nm}$ -thick CoFe film and capping layer were then deposited on this switched surface using the same process described in the Methods section. The magnetic state of the CoFe layer was then imaged at the Co  $L$ -edge using X-ray magnetic circular dichroism (XMCD)-photoemission electron microscopy (PEEM) (details of measurements are described in the Methods section) (Fig. 3b). The ferromagnetic Co image taken at  $0^\circ$  incident angle (Fig. 3b) exhibits two distinct intensity scales (contrasts), corresponding to in-plane ferromagnetic domains aligned horizontally left or right (black) and vertically up (grey) relative to the image. For the experimental geometry shown in Fig. 3b, we cannot distinguish left from right horizontally

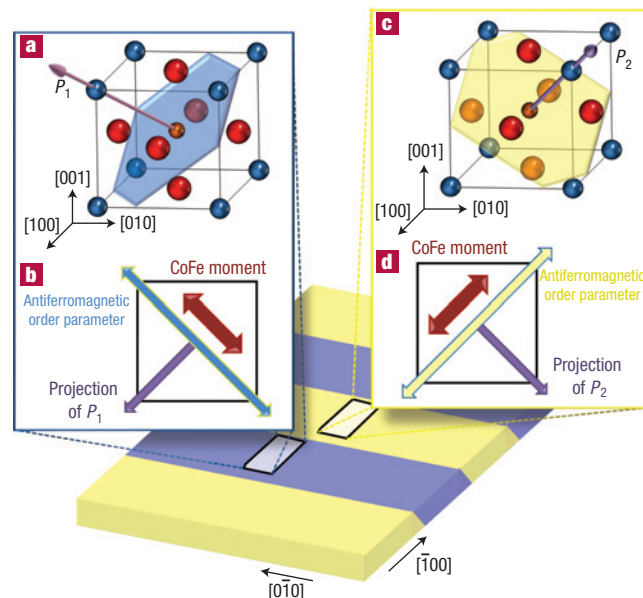


**Figure 4** Mechanism of coupling in CoFe/BFO heterostructures. **a–d**, Schematic diagrams of two adjacent domains in the [001]-oriented BFO crystal (**a,c**), in which the [111] polarization directions as well as the antiferromagnetic plane (that is perpendicular to this  $P$  direction) are identified, and the corresponding projections of the polarization direction, the antiferromagnetic plane onto the [001] and the corresponding  $M$ -directions in the CoFe layer (**b,d**).

oriented ferromagnetic domains. These domains can be resolved, however, on rotation of the sample (Fig. 3c). Rotation of the sample relative to the incoming right-circularly polarized light reveals that indeed we have only two distinct orientations for the magnetic domains in Fig. 3b. Rotating by both  $-45^\circ$  and  $45^\circ$  and focusing on the magnified area in the orange square (Fig. 3b), we have determined that the CoFe forms domains that are aligned  $90^\circ$  with respect to each other and that the local magnetic domain structure follows the ferroelectric domain structure of BFO exactly. These images provide the first direct microscopic evidence of exchange coupling between a ferromagnet and a multiferroic at this length scale ( $\sim 200\ \text{nm}$ ). Moreover, the highly correlated nature of the ferroelectric and magnetic domain structures suggests that electric control of ferromagnetism might indeed be possible.

To interpret the interrelationship between the PFM and PEEM images, we need to first understand the nature of antiferromagnetism in BFO. Figure 4a,c shows schematic diagrams of two adjacent domains in a 001-oriented BFO film, in which the [111] polarization directions as well as the antiferromagnetic plane (that is perpendicular to this polarization direction) are identified. The corresponding projections of the polarization direction and the antiferromagnetic plane onto the (001) are illustrated in Fig. 4b,d for each domain, respectively. The polarization directions project as  $\langle 110 \rangle$  directions, whereas the antiferromagnetic plane projects as a  $\langle 110 \rangle$  direction. Finally, the corresponding magnetization directions in the CoFe layer are also shown in Fig. 4b,d. The PEEM and PFM data presented in Fig. 3 strongly indicate a collinear coupling between the CoFe magnetization direction and the projection of the antiferromagnetic plane in BFO. Although it is possible that epitaxial strain breaks the degeneracy of magnetization in the {111} and consequently leads to an easy magnetic direction in the BFO (refs 9,20) (to which the

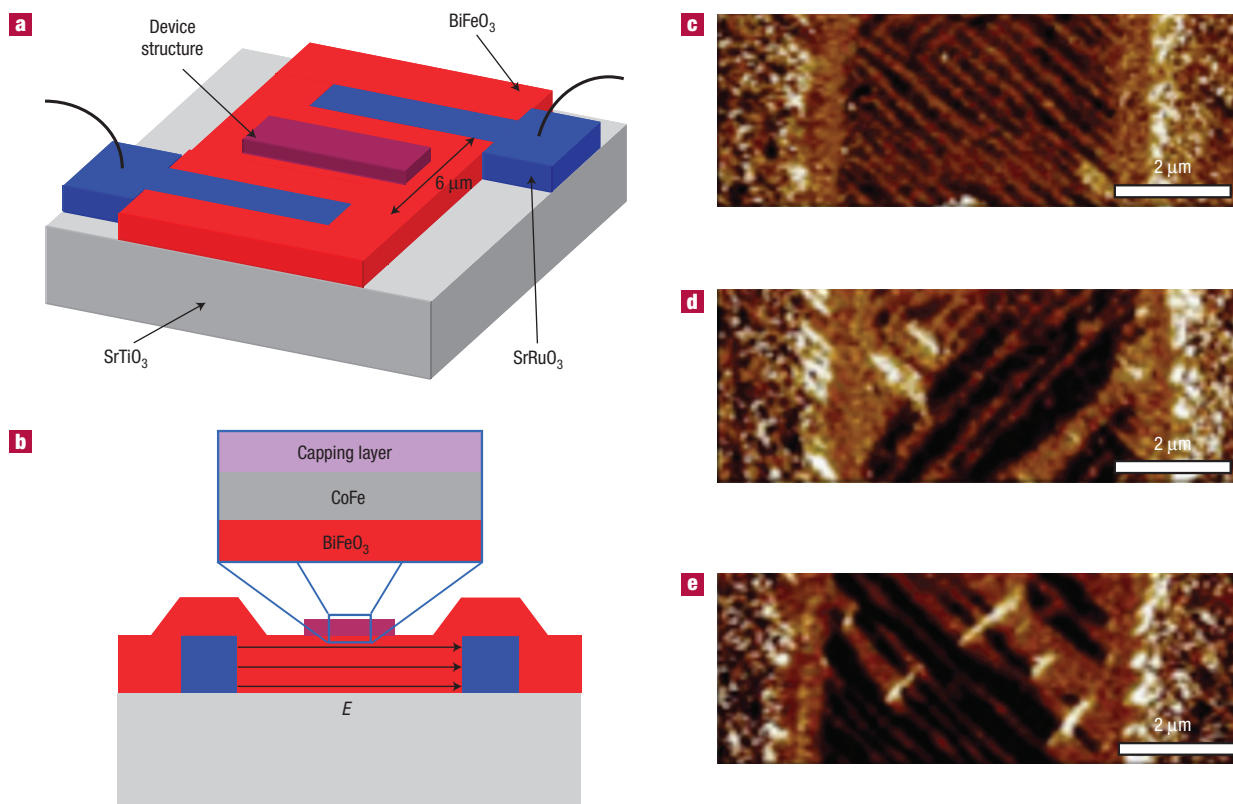


**Figure 5** Dynamic switching device structure. **a,b**, Three-dimensional (**a**) and cross-sectional (**b**) schematic diagrams of the coplanar epitaxial electrode device showing the structure that will enable controlled ferroelectric switching and electrical control of local ferromagnetism in the CoFe features. **c–e**, In-plane PFM images showing the ferroelectric domain structure for a device in the as-grown state (**c**), after the first electrical switch (**d**) and after the second electrical switch (**e**).

magnetization in the CoFe can couple), it seems that this is not a necessary condition for the existence of coupling between the ferromagnet and the antiferromagnet.

In turn, it is important to ask what happens to the antiferromagnetism as the ferroelectric order parameter is electrically switched. On the basis of the rhombohedral structure of BFO, a (001)-oriented BFO film can have eight possible polarization directions pointing along the pseudocubic (111). On application of an electric field, it is known that five possible ferroelectric or ferroelastic switching events can occur<sup>7</sup>. These include the four ferroelastic switching events—71° in-plane and out-of-plane switching events and the corresponding 109° switching events—as well as a ferroelectric 180° polarization reversal. These switching events can be visualized as combinations of both in-plane and out-of-plane rotations of the polarization direction. Visualizing such switching events as rotations of the projection of the polarization on the (001) (the film plane) enables us to identify two switching events—a 71° in-plane switching event (consisting of a 0° change in the out-of-plane and a 90° change in the in-plane component of polarization) and a 109° out-of-plane switching event (a combination of a 90° change in both the out-of-plane and in-plane components of the polarization)—that give rise to corresponding rotations of the antiferromagnetic order in BFO. Our previous work<sup>9</sup>, and recent work by LeBeugle *et al.*<sup>19</sup> on single crystals of BFO, have demonstrated that such changes in the ferroelectric order are indeed accompanied by a corresponding rotation of the antiferromagnetic order. Thus, the scenario described here provides a pathway to controllably change magnetism with the application of an electric field to the multiferroic.

Our approach to control ferromagnetism with an electric field is schematically described in Fig. 5a,b, which illustrates a simple device structure that enables the switching of ferroelectric stripe domains by a 71° in-plane switching process. The device consists of in-plane electrodes (blue in Fig. 5a,b) that enable the application of in-plane electric fields to the BFO layer (red in Fig. 5a,b). Details of the device fabrication process are listed in the Methods section. It is important to note that as a consequence of the etch process used to define such a test structure, the overgrowth of BFO between the SRO in-plane contacts leads to a higher average surface roughness  $\sim 1\text{--}4$  nm. Consequently, in the present set of experiments, samples with BFO roughness greater than 2.5 nm were excluded (because the ferromagnetic layer is of the same order of thickness). The magnetic state of the CoFe (purple in Fig. 5a,b) and changes in this state as a consequence of changes in the BFO layer were imaged using XMCD-PEEM.

Figure 5c–e shows in-plane PFM images of the BFO layer for this device structure in the as-grown state (Fig. 5c), after the first electrical switch (Fig. 5d) and after the second electrical switch (Fig. 5e). These in-plane PFM images reveal the presence of a set of two stripe-like domains (black and brown contrast in the images) running at 45° to the SRO in-plane contacts. In the as-grown state (Fig. 5c), we see the stripes running down from left to right, but on electrical poling, we observe that the stripes change by 90° in-plane and are now running up from left to right (Fig. 5d), and finally on application of the opposite electric field, we can switch the domains back to the same direction as the as-grown state (Fig. 5e). This series of images gives direct evidence of our ability to electrically switch the in-plane component in BFO by 90° in a repeatable fashion.

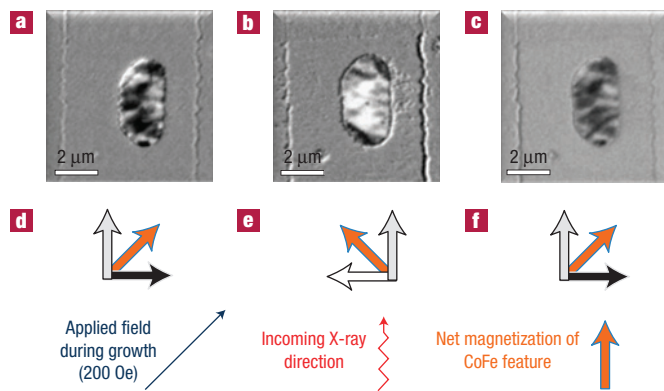


**Figure 6** Electrical control of local ferromagnetism. **a–c**, XMCD-PEEM images taken at the Co *L*-edge revealing the ferromagnetic domain structure of the CoFe features in such a coplanar electrode device structure in the as-grown state (**a**), after the first electrical switch (**b**) and after the second electrical switch (**c**). **d–f**, Schematic descriptions of the observed magnetic contrast (grey, black and white) in the corresponding XMCD-PEEM images, respectively. Application of an electric field is found to rotate the next magnetization of the structures by 90°. The direction of the applied growth field and the incoming X-ray direction are labelled as well.

Corresponding PEEM images taken at the Co *L*-edge for CoFe features grown on such a BFO surface in the as-grown state, after the first electrical switch and following a second electrical switch are shown in Fig. 6a–c, respectively. Interpretation of the various PEEM contrasts for Fig. 6a–c and the average magnetic state of these features is shown in Fig. 6d–f. On application of an electric field to the underlying BFO layer, we observe changes in the ferromagnetic contrast of the CoFe features. Similar changes were observed in multiple features on multiple samples (10 at the time of writing this paper). It is pertinent to ask the question: what do these changes in contrast mean within the framework of the data that we presented in Figs 3 and 4? Analysis of the intensity distribution in the PEEM image enables us to reveal the direction of the local magnetization in the CoFe. Our observations indicate that the average magnetization direction in the ferromagnet rotates by 90° on the application of the electric field (compare Figs 6a,d to 6b,e). On switching the BFO once again, the average magnetization direction changes back to the original state (Fig. 6c,f). We note that these promising results notwithstanding, our observations are still early in our understanding of the details of the coupling in such heterostructures. Furthermore, the exact details of factors such as the BFO surface roughness, the shape and thickness of the CoFe layer, the magnitude of the applied magnetic field during the growth process and most importantly the magnitude of the coupling energy between the antiferromagnet and ferromagnet in relation to other energy scales in this coupled system (magnetostatic energy, magnetocrystalline anisotropy energy) need to be carefully examined in future experimental and theoretical studies. In summary, we have presented direct evidence for electric-field control of local ferromagnetism through the coupling between multiferroic BFO and a ferromagnet.

## METHODS

Epitaxial thin films of BFO and SRO were grown using pulsed laser deposition at 700 °C in 100 mtorr of oxygen. Following deposition of the BFO, the

films were cooled in 1 atm of oxygen to room temperature. The samples were then transported to a vacuum sputtering system with a base pressure of  $\sim 5 \times 10^{-9}$  torr where the ferromagnetic metal and capping films were grown. Growth of the CoFe films in an applied field,  $H_{\text{growth}} = 200$  Oe, enables us to induce a uniaxial anisotropy in the system.

The coplanar epitaxial electrode structures are created by first growing an epitaxial film of the electrode material SRO ( $\sim 50$  nm in thickness) at 700 °C. Following the growth of the blanket SRO layer, photolithography is used to define a set of electrodes and a ground electrode. The surrounding SRO material is then etched using an ion milling process down to the underlying substrate, leaving only the defined SRO electrode structures on the sample. Following this step, a BFO film of between 100 and 150 nm is grown using the same process noted earlier. Following growth of the BFO layer, the films are transported to the ultrahigh-vacuum metal deposition system for deposition of the metallic species. Another photolithography process is used to create a series of CoFe features and ion milling is used to etch away the surrounding CoFe film down to the underlying BFO layer. The end features have been designed to encompass a number of different width-to-length aspect ratios.

XMCD-PEEM measurements were completed at various energies and polarizations of focused X-rays that were incident on the sample at an angle of 30° from the surface and formed a spot approximately 30  $\mu\text{m}$  in diameter. Imaging was done by tuning the photon energy to the Co *L*-edge ( $\sim 780$  eV) and using right- or left-handed circularly polarized radiation enabled imaging of the ferromagnetic CoFe domain structure by exploiting the XMCD effect at the Co *L*<sub>3</sub>- and *L*<sub>2</sub>-edges.

Received 26 February 2008; accepted 2 April 2008; published 27 April 2008.

## References

- Wang, J. *et al.* Epitaxial BiFeO<sub>3</sub> multiferroic thin film heterostructures. *Science* **299**, 1719–1722 (2003).
- Eerenstein, W., Mathur, N. D. & Scott, J. F. Multiferroic and magnetoelectric materials. *Nature* **442**, 759–765 (2006).
- Ramesh, R. & Spaldin, N. A. Multiferroics: progress and prospects in thin films. *Nature Mater.* **6**, 21–29 (2007).
- Kiselev, S. V., Ozerov, R. P. & Zhdanov, G. S. Detection of magnetic order in ferroelectric BiFeO<sub>3</sub> by neutron diffraction. *Sov. Phys. Dokl.* **7**, 742–744 (1963).
- Teague, J. R., Gerson, R. & James, W. J. Dielectric hysteresis in single crystal BiFeO<sub>3</sub>. *Solid State Commun.* **8**, 1073–1074 (1970).
- Chu, Y.-H. *et al.* Domain control in multiferroic BiFeO<sub>3</sub> through substrate vicinality. *Adv. Mater.* **19**, 2662–2666 (2007).
- Zavaliche, F. *et al.* Multiferroic BiFeO<sub>3</sub> films: Domain structure and polarization dynamics. *Phase Transit.* **79**, 991–1017 (2006).
- Ederer, C. & Spaldin, N. A. Weak ferromagnetism and magnetoelectric coupling in bismuth ferrite. *Phys. Rev. B* **71**, 060401(R) (2005).
- Zhao, T. *et al.* Electrical control of antiferromagnetic domains in multiferroic BiFeO<sub>3</sub> films at room temperature. *Nature Mater.* **5**, 823–829 (2006).
- Meiklejohn, W. H. & Bean, C. P. New magnetic anisotropy. *Phys. Rev.* **102**, 1413–1414 (1956).
- Nogués, J. & Schuller, I. K. Exchange bias. *J. Magn. Magn. Mater.* **192**, 203–232 (1999).
- Dho, J. & Blamire, M. G. Competing functionality in multiferroic YMnO<sub>3</sub>. *Appl. Phys. Lett.* **87**, 252504 (2005).
- Marti, X. *et al.* Exchange bias between magnetoelectric YMnO<sub>3</sub> and ferromagnetic SrRuO<sub>3</sub> epitaxial films. *J. Appl. Phys.* **99**, 08P302 (2006).
- Dho, J., Qi, X., Kim, H., MacManus-Driscoll, J. L. & Blamire, M. G. Large electric polarization and exchange bias in multiferroic BiFeO<sub>3</sub>. *Adv. Mater.* **18**, 1445–1448 (2006).
- Béa, H. *et al.* Tunnel magnetoresistance and robust room temperature exchange bias with multiferroic BiFeO<sub>3</sub> epitaxial thin films. *Appl. Phys. Lett.* **89**, 242114 (2006).
- Martin, L. W. *et al.* Room temperature exchange bias and spin valves based on BiFeO<sub>3</sub>/SrRuO<sub>3</sub>/SrTiO<sub>3</sub>/Si (001) heterostructures. *Appl. Phys. Lett.* **91**, 172513 (2007).
- Borisov, P., Hochstrat, A., Chen, X., Kleman, W. & Binek, C. Magnetoelectric switching of exchange bias. *Phys. Rev. Lett.* **94**, 117203 (2005).
- Laukhin, V. *et al.* Electric-field control of exchange bias in multiferroic epitaxial heterostructures. *Phys. Rev. Lett.* **97**, 227201 (2006).
- LeBeugle, D. *et al.* Electric-field-induced spin flop in BiFeO<sub>3</sub> single crystals at room temperature. Preprint at <http://arxiv.org/abs/0802.2915> (2008).
- Nolting, F. *et al.* Direct observation of the alignment of ferromagnetic spins by antiferromagnetic spins. *Nature* **405**, 767–769 (2000).

## Acknowledgements

The work at Berkeley is supported by the Director, Office of Science, Office of Basic Energy Sciences, Materials Sciences Division of the US Department of Energy under contract No. DE-AC02-05CH1123. The authors from both Berkeley and Stanford would also like to acknowledge the support of the Western Institute of Nanoelectronics and acknowledge the support of the National Center for Electron Microscopy, Lawrence Berkeley National Laboratory.

## Author information

Reprints and permission information is available online at <http://npg.nature.com/reprintsandpermissions>. Correspondence and requests for materials should be addressed to L.W.M.